



OPEN ACCESS

EDITED BY

Yanqiu Zhang,
Changzhou University, China

REVIEWED BY

Weiyu Shi,
Southwest University, China
Nataliya Yurkevich,
Institute of Petroleum Geology and
Geophysics (RAS), Russia
Tong Ouyang,
Xiamen University, China

*CORRESPONDENCE

Kengo Nakamura,
nakamurakengo@mail.saitama-u.ac.jp
Jiajie Wang,
wang.jiajie.e4@tohoku.ac.jp
Noriaki Watanabe,
noriaki.watanabe.e6@tohoku.ac.jp

SPECIALTY SECTION

This article was submitted to Soil
Processes,
a section of the journal
Frontiers in Environmental Science

RECEIVED 13 October 2022

ACCEPTED 14 November 2022

PUBLISHED 25 November 2022

CITATION

Yoshioka R, Nakamura K, Sekiai R,
Wang J and Watanabe N (2022),
Effectiveness and characteristics of
atmospheric CO₂ removal in croplands
via enhanced weathering of industrial
Ca-rich silicate byproducts.
Front. Environ. Sci. 10:1068656.
doi: 10.3389/fenvs.2022.1068656

COPYRIGHT

© 2022 Yoshioka, Nakamura, Sekiai,
Wang and Watanabe. This is an open-
access article distributed under the
terms of the [Creative Commons
Attribution License \(CC BY\)](https://creativecommons.org/licenses/by/4.0/). The use,
distribution or reproduction in other
forums is permitted, provided the
original author(s) and the copyright
owner(s) are credited and that the
original publication in this journal is
cited, in accordance with accepted
academic practice. No use, distribution
or reproduction is permitted which does
not comply with these terms.

Effectiveness and characteristics of atmospheric CO₂ removal in croplands via enhanced weathering of industrial Ca-rich silicate byproducts

Rina Yoshioka¹, Kengo Nakamura^{1,2*}, Ryota Sekiai¹,
Jiajie Wang^{1*} and Noriaki Watanabe^{1*}

¹Department of Environmental Studies for Advanced Society, Graduate School of Environmental Studies, Tohoku University, Sendai, Japan, ²Geotechnical and Geosphere Research Group, Saitama University, Saitama, Japan

Enhanced weathering of industrial Ca-rich silicate byproducts in croplands is potentially profitable for large-scale atmospheric CO₂ removal; during the weathering process, CO₂ dissolves to form HCO₃⁻ and CO₃²⁻ in alkaline soil pore water, which eventually flows into the ocean. However, the effectiveness of such systems is still in doubt, owing to the unrealistic models used for prediction and the insufficient consideration of the dynamic influences of soils on fluid chemistry. We determined the effectiveness of such systems for atmospheric CO₂ removal, along with their characteristics, through a set of batch- and flow-through-type laboratory experiments, using andosol and decomposed granite soil as agricultural and non-agricultural soils, respectively, and Portland cement, steelmaking slag, and coal fly ash as industrial byproducts. The results of the batch-type experiments demonstrated that agricultural soils were suitable for CO₂ removal, owing to their moderately high pH and Ca concentrations in pore water that prevented intensive calcium carbonate precipitation. The flow-through experiments demonstrated that a higher Ca-content byproduct can have a large atmospheric CO₂ removal capacity. However, the magnitude of CO₂ removal and its time-dependent behavior were difficult to predict because they were not in conjunction with the changes in the average pH value. This indicated that the diffusive transport of CO₂ from the atmosphere-soil interface to deeper soils was more complex than expected. Maximizing CO₂ removal requires a better understanding of the diffusive transport of CO₂ through gas-filled pore spaces, created by unsteady-state air-water two-phase flow, due to intermittent rainfall.

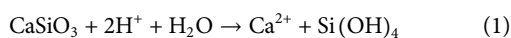
KEYWORDS

atmospheric CO₂ removal, cropland, enhanced weathering, industrial Ca-rich byproduct, sustainability

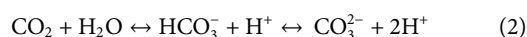
1 Introduction

Based on the Paris Agreement, the United Nations Intergovernmental Panel on Climate Change (IPCC) aims to limit anthropogenic global warming; for this, it is imperative to consider large-scale atmospheric carbon dioxide (CO₂) removal (Hansen et al., 2017; Rockström et al., 2017; IPCC 2018; Bach et al., 2019). The atmospheric CO₂ removal technologies recently developed focus on the use of soil and vegetation for atmospheric CO₂ removal (Green et al., 2019; Humphrey et al., 2021; Terrer et al., 2021; Zeng et al., 2022). In these reports, enhanced weathering of calcium (Ca) and/or magnesium (Mg) silicate rocks/minerals applied in croplands has shown potential for atmospheric CO₂ removal. Such enhanced weathering also has the possible co-benefits of improved food and soil security and reduced ocean acidification (Kantola et al., 2017; Zhang G. et al., 2018; Beerling et al., 2018, 2020; Bach et al., 2019; Goll et al., 2021).

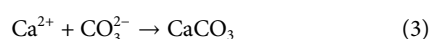
A recent study by Beerling et al. (2020) suggested the possibility of large-scale profitable atmospheric CO₂ removal, through the enhanced weathering of industrial Ca/Mg-rich silicate byproducts in croplands. Industrial silicate byproducts, including steelmaking slag, waste cement, and coal fly ash (Lam et al., 2000; Jorat et al., 2020; Abdel-Gawwad et al., 2021; Klemettinen et al., 2021), have been used in the agricultural sector to supplement minerals to the soil (Das et al., 2019). Based on a one-dimensional (1D) vertical reactive transport model simulation, Beerling et al. (2020) estimated that an average global atmospheric CO₂ removal of 0.5–2 Gt/year may be achieved by applying enhanced weathering in various countries, such as China, India, Brazil, and the United States of America (United States), with the costs being approximately USD 80–180 per ton of CO₂. In this CO₂ removal process, CO₂ is captured as HCO₃⁻ and CO₃²⁻ in alkaline soil pore water, resulting from the fast dissolution of fine-grained Ca/Mg-rich silicates that eventually flow into the ocean. For instance, calcium silicate (CaSiO₃) dissolves in soil pore water, which can be expressed as the following equation:



In this reaction, protons (H⁺) are consumed, facilitating the dissolution of atmospheric CO₂ into pore water. This reaction can be expressed as follows:



However, in this atmospheric CO₂ removal process, carbonate minerals, such as CaCO₃, may be generated under conditions of high pH (i.e., low solubility of carbonate minerals in water) and high concentrations of Ca²⁺/Mg²⁺ and CO₃²⁻, as shown in Eq. 3:



Ca- and Mg-rich silicate materials have another role in CO₂ removal; they serve as conditioners for Ca- and Mg-depleted soils, respectively. Therefore, intensive formation of carbonate minerals is not desirable for croplands, because they reduce the readily available Ca/Mg for plants. Additionally, this may result in the dissolution of carbonate minerals, consequently resulting in the release of CO₂ into the atmosphere; notably, this may occur unless the pH of the pore water is high enough to limit carbonate dissolution.

Croplands have been considered as good candidates for the application of large-scale profitable atmospheric CO₂ removal technologies (Beerling et al., 2020). However, the existing studies do not determine the properties of croplands that contribute to atmospheric CO₂ removal and the CO₂ removal pathways and mechanisms in croplands. Moreover, the dynamic influences of cropland soils on fluid chemistry, such as the kinetics of pH buffering and cation exchange, have been rarely considered (Russell et al., 2006; Nelson and Su 2010; Torrent et al., 2015; Wuenschel et al., 2015; Baquy et al., 2018; Dai et al., 2018). The steady-state single-phase (water) flow in a soil, with a static distribution of gas-phase CO₂ concentration, is not realistic, as water inputs to croplands by rainfall intermittently cause an unsteady-state air–water two-phase flow in soils that have a dynamic distribution of gas-phase CO₂ concentration.

Notably, it is unclear whether agricultural soils can quickly achieve moderately high pH and effective Ca and Mg concentrations in soil pore water, required to prevent the intensive precipitation of carbonate minerals, even when highly reactive Ca/Mg-rich silicate materials react with the pore water. It is also unclear whether the CO₂ removal behavior can be predicted based only on the average changes in the chemistry of the pore water, while neglecting the spatially variable distribution of the gas phase, due to the unsteady-state air–water two-phase flow. In this study, we aimed to clarify these points through a set of batch- and flow-through-type laboratory experiments on atmospheric CO₂ removal, using powders of Portland cement, steelmaking slag, and coal fly ash (as representatives of industrial Ca-rich silicate materials) and andosol and decomposed granite (DG) soil (as representatives of agricultural and non-agricultural soils). Batch-type experiments conducted using both agricultural and non-agricultural soils revealed the effectiveness of applying silicate materials, particularly to croplands. Flow-through-type experiments conducted using agricultural soil, through which vertical water flow occurred intermittently, were used to investigate the characteristics of atmospheric CO₂ removal.

2 Materials and methods

2.1 Soils and Ca-rich silicate materials

In this study, andosol and DG soils, which form naturally and are commercially available in Japan, were used as representatives of

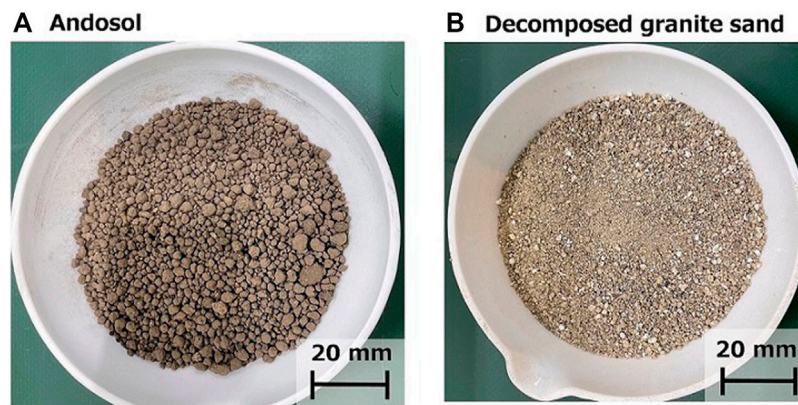


FIGURE 1

Photos of (A) andosol and (B) decomposed granite soil sample before sieving; sieving was carried out to adjust the particle size for the experiment.

TABLE 1 Major element concentrations and total organic carbon (TOC) in the andosol, decomposed granite (DG) soil, Portland cement, steelmaking slag, and coal fly ash samples used in this study.

	Andosol	DG soil	Cement	Slag	Fly ash
Na ₂ O (wt%)	1.5	3.2	0.6	0.5	0.7
MgO (wt%)	1.5	0.2	3.3	4.0	0.9
Al ₂ O ₃ (wt%)	17.5	17.0	7.9	11.8	19.6
SiO ₂ (wt%)	64.0	79.0	23.4	31.5	72.4
P ₂ O ₅ (wt%)	0.6	0.1	0.1	0.0	0.8
K ₂ O (wt%)	1.4	4.8	0.2	0.3	1.3
CaO (wt%)	2.1	0.6	57.2	43.7	3.6
TiO ₂ (wt%)	0.6	0.2	0.4	0.7	1.1
Fe ₂ O ₃ (wt%)	6.4	1.9	1.7	0.1	4.7
Total (wt%)	95.6	107.0	94.8	92.6	105.1
TOC (mg/g)	47.0	1.2	0.9	0.8	12.0

agricultural and non-agricultural soils, respectively (Figure 1). Andosol, known as Kuroboku soil in Japan, mainly consists of volcanic ash and humus. It is distributed over ~31% of Japan's land area, and covers ~47% of the country's crop fields. Table 1 lists the major element concentrations and total organic carbon (TOC) of the soils used in this study.

The elemental concentration and TOC of the soils and Ca-rich silicate materials were determined using an energy dispersive X-ray fluorescence analyzer (EDX-720, Shimadzu Corporation, Kyoto, Japan) and an organic elemental analyzer (vario MACRO cube, Elementar, Germany). In general, both andosol and DG soils are particularly rich in Si and Al. However, andosols have higher TOC concentrations, as the soil contains substantial amounts of humus, indicating high pH buffering and cation exchange abilities, which contribute to atmospheric CO₂ removal, without intensive CaCO₃ precipitation. X-ray diffraction (XRD) analysis was conducted to analyze the soils and Ca-rich silicate materials using an X-ray

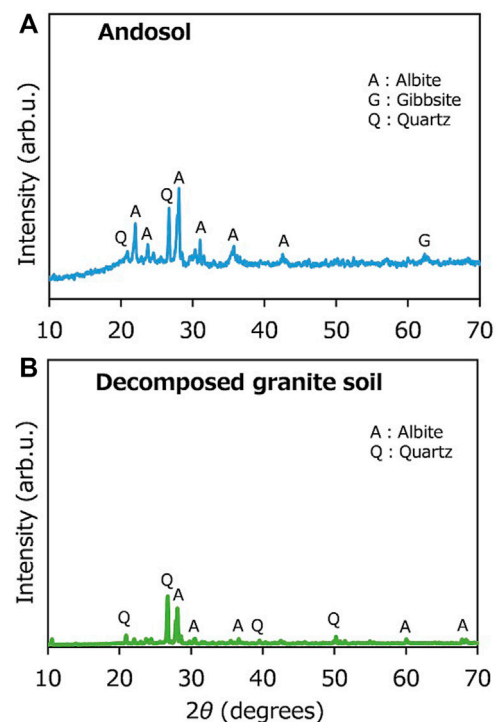


FIGURE 2

X-ray diffraction patterns observed in the experiment for (A) andosol and (B) decomposed granite soil.

diffractometer (MiniFlex, Rigaku Corporation, Japan) with Cu-K α radiation, from 10° to 70° (with a step size of 2 θ), at 40 kV and 15 mA. The XRD patterns shown in Figure 2 reveal that the dominant crystal phases are albite (NaAlSi₃O₈), gibbsite (Al(OH)₃), and quartz (SiO₂) for andosol and albite and quartz for DG soil, indicating no or negligible amounts of carbonate minerals in the two

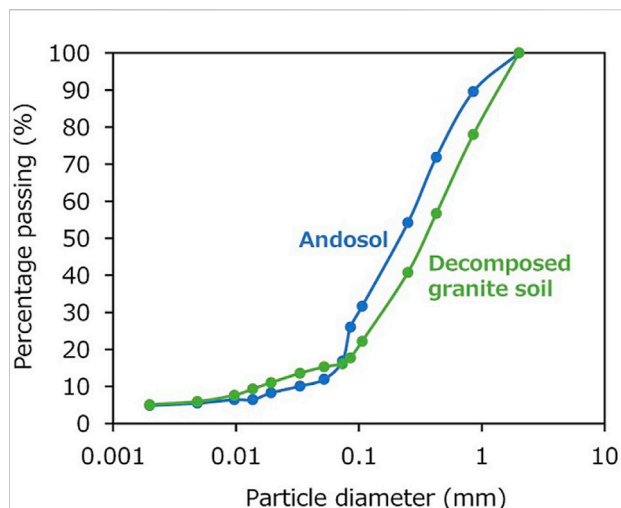


FIGURE 3

Particle size distribution curves for andosol and decomposed granite soil after sieving, to adjust the particle size of the soil samples for the experiment.

types of soils. Both soils were air-dried, and particles of sizes <2 mm, segregated by sieving, were selected for the experiments. Figure 3 portrays the particle size distributions for both soils.

In this experimental study, Portland cement, steelmaking slag, and coal fly ash were used as representative Ca-rich industrial byproducts (Figure 4). These materials were air-dried and used in the experiments without particle size adjustment.

2.2 Experimental system, procedures, and conditions

2.2.1 Batch type experiment for atmospheric CO₂ removal

In the batch-type experiment, we used 600 ml of Milli-Q water (pH ~7), with/without 120 g of soil, and/or 6 g of Ca-rich silicate material was put into a cylindrical polypropylene tank (wall thickness: 0.2 mm, outer diameter and height: 11.5 cm); all contents were mixed well, using a stainless-steel stirrer, at 25°C for 2 h, during which the pH of the suspension was measured every 10 min, using a pH meter (HM-31P, DKK-TOA Corporation, Japan). Table 2 lists the combinations of soil and Ca-rich silicate materials used in each experiment.

After 2 h of mixing, a part of the solution suspension was filtered through a 0.45- μ m membrane to obtain the solution, and the concentrations of Al, Si, and Ca (which were high in the raw solid materials) were measured using an inductively coupled plasma optical emission spectrometer (ICP-OES) (Agilent 5,110, Agilent Scientific Instruments, United States). The concentrations of TOC and inorganic carbon (IC) were measured using a TOC analyzer (Sensing eye 332, Techno

TABLE 2 Combination of soil and Ca-containing silicate material in each batch-type experiment.

Experiment	Soil	Ca-rich silicate material
Run 1	-	-
Run 2	Andosol	-
Run 3	Andosol	Portland cement
Run 4	Andosol	Steelmaking slag
Run 5	Andosol	Fly ash
Run 6	Decomposed granite soil	-
Run 7	Decomposed granite soil	Portland cement
Run 8	Decomposed granite soil	Steelmaking slag
Run 9	Decomposed granite soil	Fly ash
Run 10	-	Portland cement

Morioka Co., Ltd, Yamagata, Japan). Higher TOC and IC values reflect higher concentrations of organic compounds eluted from the raw solid materials into the solution and the CO₂ species absorbed from the atmosphere into the solution. Thermogravimetry (TG) in air was also conducted on the soils. Additionally, after the experiment, selected mixtures of soil and Ca-rich materials were dried at 80°C for 24 h, to confirm CaCO₃ precipitation; for this, we used a differential thermogravimetric analyzer (Thermo plus EVO TG 8120, Rigaku Corporation, Tokyo, Japan), for a range of temperatures from room temperature (25°C) to 1,000°C, at a heating rate of 10°C/min (Wang et al., 2022). All experiments were only conducted for once, but the measurements were conducted for three times for ICP-OES, with a good reproducibility within a margin of error of 3%.

2.2.2 Flow-through type experiment for atmospheric CO₂ removal

Two kinds of flow-through type experiments were conducted at 25°C, by sprinkling Milli-Q water on the andosol sample packed in a cylindrical container having a discharge port at its bottom, with the Ca-rich silicate material distributed uniformly on the soil surface (Figure 5). The cylindrical container was made of polypropylene and had a wall thickness of 0.5 cm, outer diameter of 12.0 cm, and outer height of 14.0 cm. We placed 600 g of commercially available natural quartz sand (particle diameter: 1.2–2.4 mm) at the bottom of the container, which served as a highly permeable layer of approximately 3 cm; the layer facilitated the sampling of different effluents for chemical analyses. Note that a filter paper was placed at the outlet port, so that the quartz sand remained inside the container. The highly permeable layer enabled the collection of all the water that passed through the soil within several minutes. Next, 600 g of andosol was placed above the quartz sand layer to form a ~9-cm-thick soil layer. Milli-Q water (400 ml, pH ~7) was sprinkled onto the soil surface to create an initial air–water two-phase condition, where

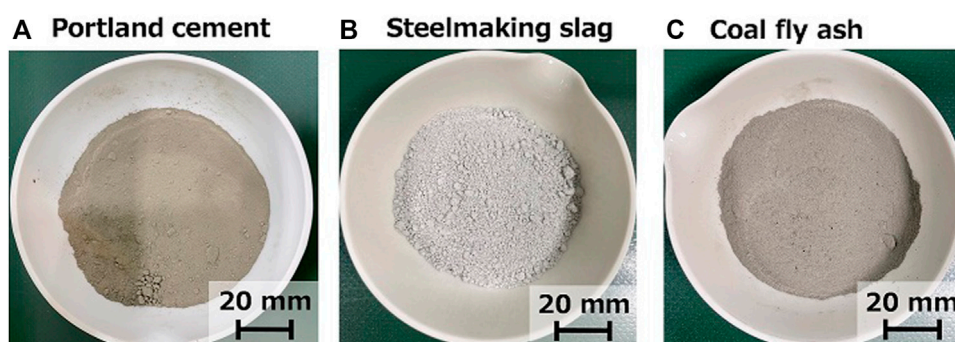


FIGURE 4
Photos of (A) Portland cement, (B) steelmaking slag, and (C) coal fly ash powders used in this study.

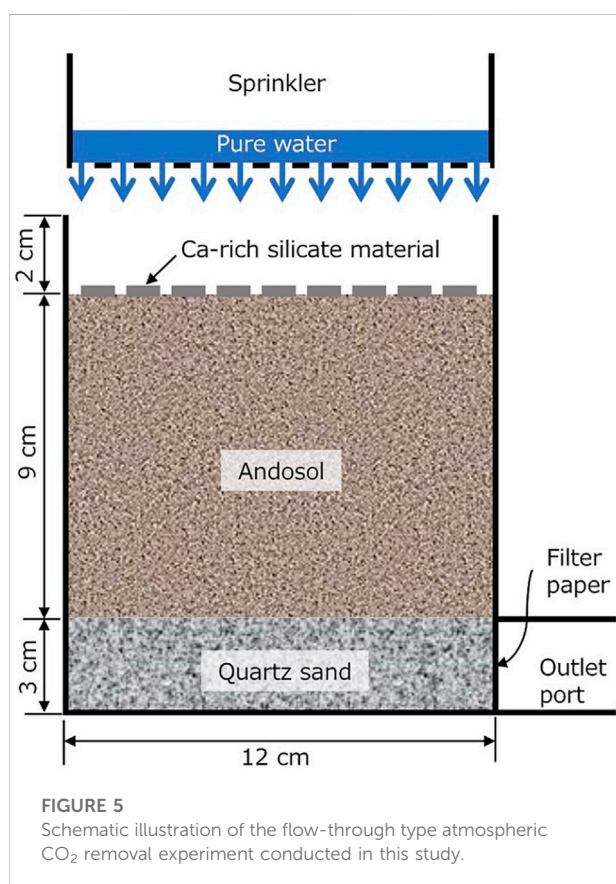


FIGURE 5
Schematic illustration of the flow-through type atmospheric CO₂ removal experiment conducted in this study.

the volumetric water saturation of the soil was approximately 50%.

After making this initial condition, one of the flow-through-type experiments was conducted in a closed 40-cm cubic box. Milli-Q water (100 ml) was sprinkled onto the soil surface at a rate of ~60 ml/s, with or without 30 g of Portland cement, steelmaking slag, or coal fly ash. After the water flow from the

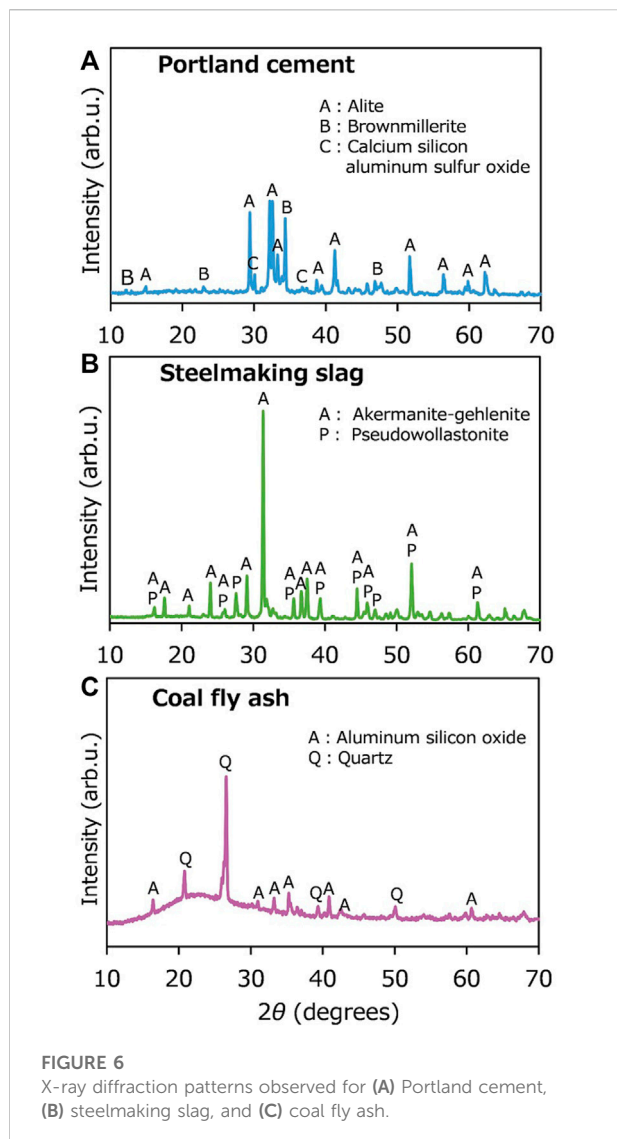
outlet port stopped, the atmospheric concentration of CO₂ in the box was measured (with the outlet port plugged every 10 min for 600 min), using a portable gas monitor (GX-6000, Riken Keiki Co., Ltd. Japan), which was also placed in a closed box.

In contrast, after developing the initial condition, the other flow-through type experiment was conducted, by intermittently sprinkling Milli-Q water, without using the closed box. Milli-Q water (100 ml) was sprinkled twice per day (10:00 and 16:00) for 5 days. For every sprinkle, the outlet port of the container was unplugged to collect effluent. Each fluid sample was first, filtered using a membrane filter and then analyzed for pH, elemental concentration, TOC, and IC.

3 Results

3.1 Effectiveness of the model for atmospheric CO₂ removal

Cement was first used to mix with andosol and DG soil in batch experiments. The composition of the cement is shown in Table 1. It was rich in Si, Ca, and Al, with the CaO concentration of 57.2 wt%. The XRD patterns shown in Figure 6 revealed that the dominant crystal phases were alite (Ca₃SiO₅), brownmillerite [Ca₂(Al,Fe)₂O₅], and calcium silicon aluminum sulfur oxide [Ca₂(Si,Al,S)O₄]. There were no or negligible amounts of carbonate minerals in cement. Figure 7A portrays the pH changes with time in the batch-type experiments for the soil samples mixed with cement. In the experiments conducted using only water (Run 1), andosol (Run 2), and DG soil suspensions (Run 6), the pH initially decreased to ~7 within 30 min and then was almost stable at pH 6.0 in Runs 1 and 2 and pH 6.5 in Run 6. In the experiment conducted using only Portland cement (Run 10), the pH was initially much higher (~pH 12) and remained almost constant throughout the experiment. In contrast, in the experiment conducted using



andosol and cement (Run 3), the pH was initially ~11, which was lower than that in Run 10, and gradually decreased to approximately 10, demonstrating the quick and substantial pH buffering ability of andosol. The increased pH due to mixing cement into andosol may enhance the leaching of humic acids from soil, resulting in a high dissolved TOC concentration, as shown in Figure 7B (Runs 2 and 3). Notably, the concentration of IC (used as a proxy of the total concentrations of CO₂ species) tended to be higher for the experiment with a high final pH, rather than being positively correlated to the pH (Figure 7A). The concentration of IC in the experiment conducted using andosol and cement (Run 3) was 3.1 times higher than that conducted using andosol alone (Run 2); for DG soil, adding cement only increased the IC in the solution by 1.7 (Runs 6 and 7).

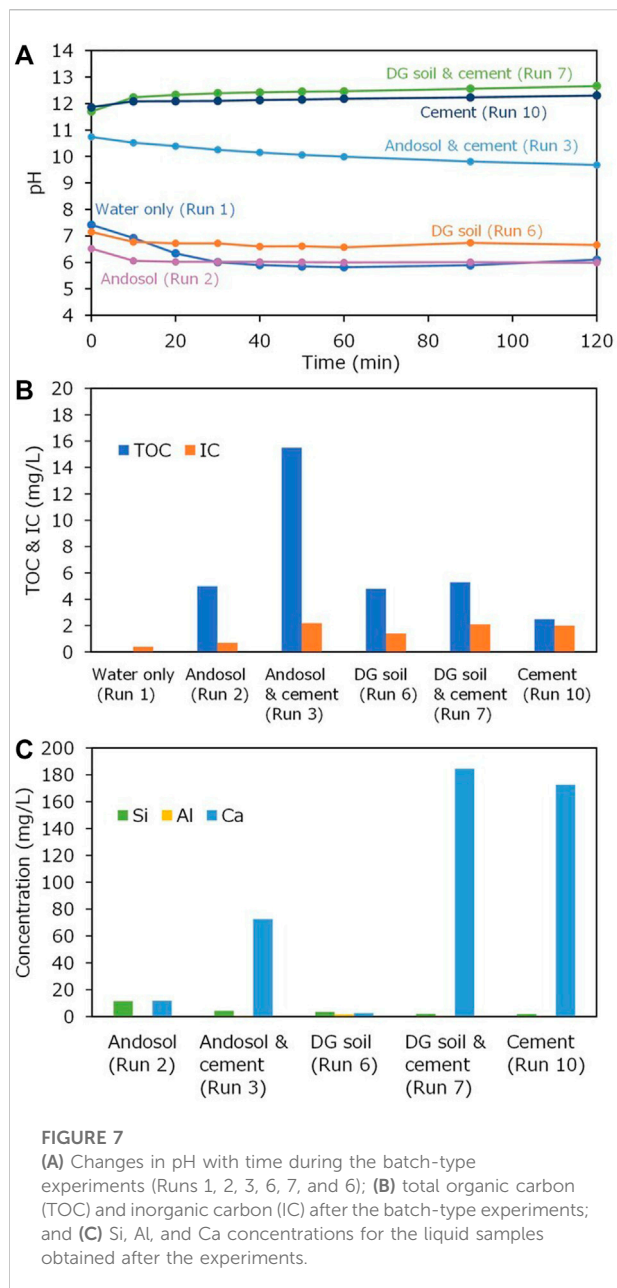
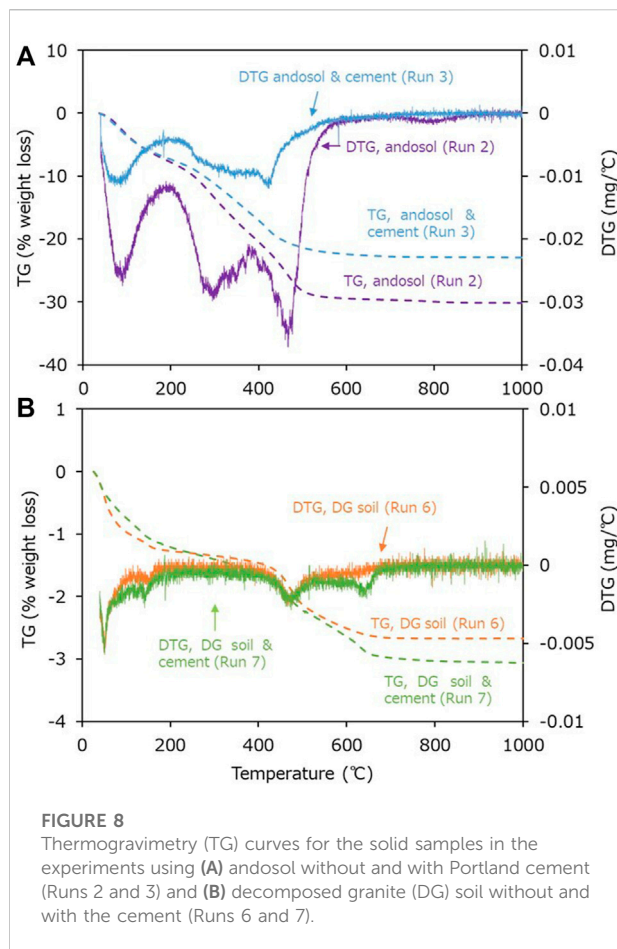
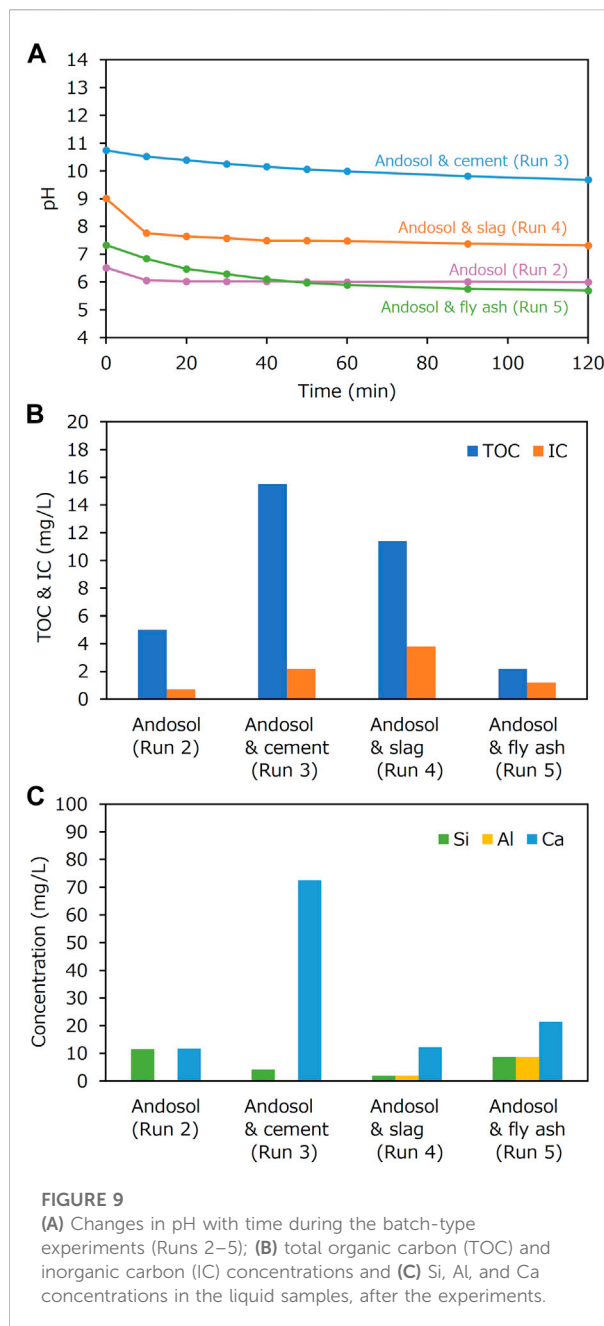


Figure 7C portrays the main elemental concentrations of the solution after the batch-type experiments. The Ca concentration in the experiment conducted using andosol and cement (Run 3) was much lower than in that conducted using cement alone (Run 10); this demonstrated the substantial cation exchange capacity of andosol, which was consistent with the results of Madeira et al. (2003). When DG soil was used, the addition of cement resulted in a higher concentration of Ca. It is implied that a large difference in the Ca concentration in the experiments conducted using andosol and DG soil with cement (Runs 3 and 7) occurred in the early stage of the experiment,



considering the large difference in the effect of cement addition on the IC concentrations in the experiments.

Figure 8A compares the TG curves for the solids collected from the experiments conducted using andosol with and without cement (Runs 2 and 3, respectively). For both samples, most weight loss occurred below 500°C, resulting in qualitatively similar TG curves. The less weight loss in the experiment conducted using andosol with cement (Run 3) may be attributed to the elution of more TOC, e.g., humic acids from andosol. In general, the decomposition of amorphous and crystalline calcium carbonates is known to occur at ~600–800°C (Kimura and Koga, 2011; Schmidt et al., 2014; Zhang J. et al., 2018; Rao et al., 2019). Therefore, we could confirm that the precipitation of calcium carbonate did not occur intensively in the experiment conducted using andosol and cement (Run 3). In contrast, the TG and DTG curves for the solids collected from the experiment conducted using DG soil with cement (Run 7) portrayed an additional weight loss at 600–700°C, which was not observed in the experiment conducted using DG soil alone (Run 6) (Figure 8B). Therefore, we could verify that precipitation of calcium carbonate occurred in the experiment conducted using DG soil and cement (Run 7). The



generation of calcium carbonates also explains the smaller increase in the IC, resulting from the addition of cement to the DG soil.

The feasibility of using steelmaking slag and coal fly ash was then investigated. As shown in Table 1, the CaO concentrations in slag and fly ash were 43.7 wt% and 3.6 wt%, respectively. The slag and fly ash samples were also rich in Si, Ca, and Al. The XRD patterns shown in Figure 6 revealed that the dominant crystal phases were åkermanite-gehlenite [$\text{Ca}_2(\text{MgAl})((\text{Si,Al})_2\text{O}_7)$] and

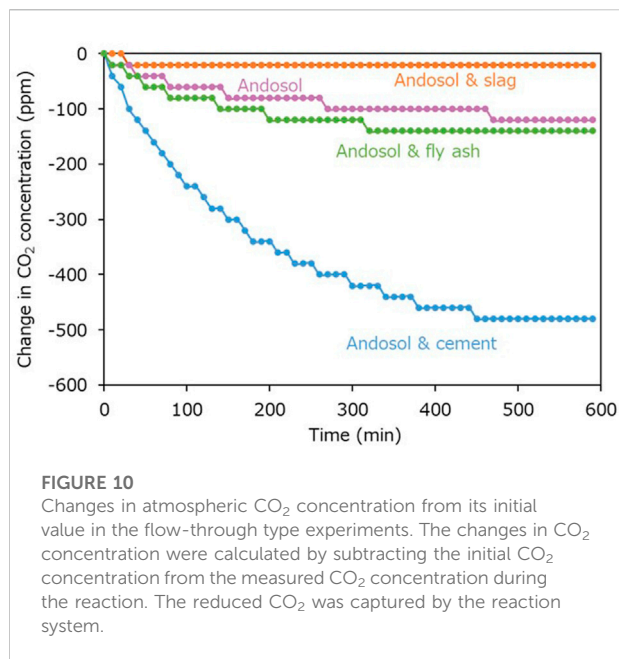


FIGURE 10

Changes in atmospheric CO_2 concentration from its initial value in the flow-through type experiments. The changes in CO_2 concentration were calculated by subtracting the initial CO_2 concentration from the measured CO_2 concentration during the reaction. The reduced CO_2 was captured by the reaction system.

pseudowollastonite (CaSiO_3) for slag, and aluminum silicon oxide ($x\text{Al}_2\text{O}_3 \cdot y\text{SiO}_2 \cdot z\text{H}_2\text{O}$) and quartz for fly ash. Carbonate minerals were not found. The effects of cement, slag and fly ash on the pH changes, TOC and IC, and elemental concentrations in the batch-type atmospheric CO_2 removal experiments conducted using andosol were compared in Figure 9 (Runs 2–5). The general trend in pH change was similar in all experiments conducted using Ca-rich silicate material, i.e., the pH portrayed a decrease in the initial stage and became stable with the reaction time. However, the pH was higher in the samples containing cement, slag, and fly ash (in this sequence). Additionally, the TOC concentration was higher at higher final pH, because of the more intensive elution of humic acids from andosol. The IC concentration was higher in the order of: samples containing slag, cement, flyash, and andosol alone (IC of 3.8, 2.2, 1.2, and 0.7 mg/L, respectively), demonstrating the effectiveness of the experiments for atmospheric CO_2 removal, for all silicate materials tested in the present study. The inconsistency between the orders of the pH and IC values may be due to the relatively larger amount of calcium carbonate formation after the addition of cement, considering the much higher Ca concentrations of the sample (Figure 9C).

Based on the above discussion, we can verify that agricultural soil with high humic acids contents, such as andosol, can quickly achieve moderately high pH and Ca concentrations in soil pore water due to the cation exchange effects, thus preventing intensive precipitation of carbonate minerals, even when highly reactive Ca-rich silicate materials, such as cement, react with the pore water. Additionally, the silicate materials tested in this study can be applied in croplands to enhance the removal of atmospheric CO_2 .

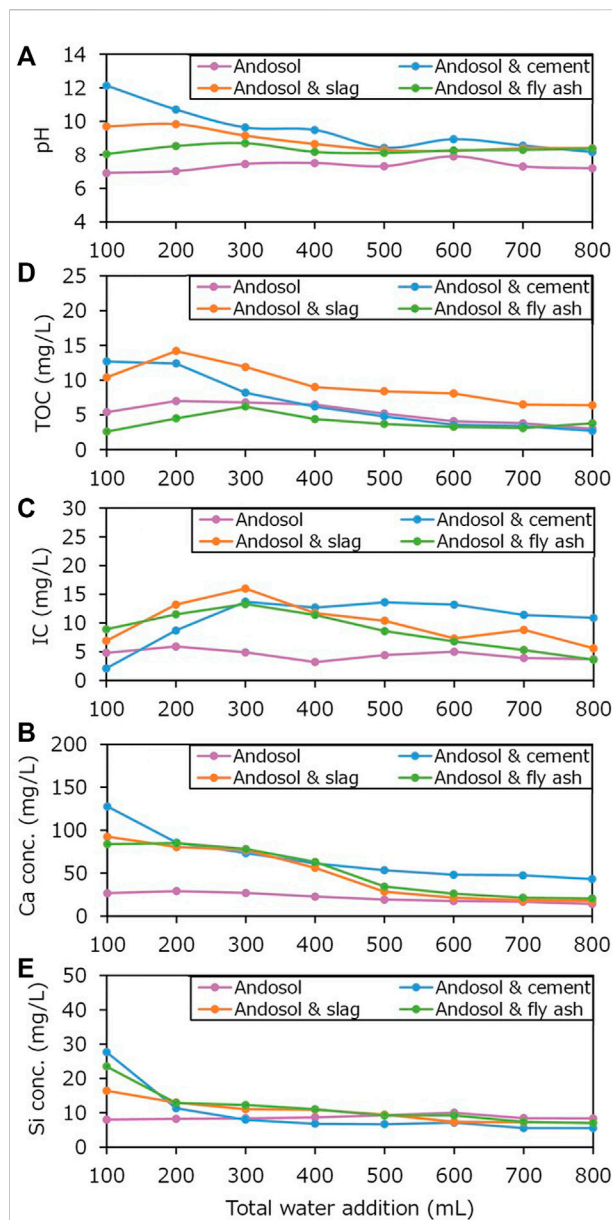


FIGURE 11

Changes in (A) pH of and (B) total organic carbon (TOC), (C) inorganic carbon (IC), and (D) Ca and (E) Si concentrations in the effluents in the flow-through type experiments, without the closed box, as a function of total water addition.

3.2 Rate-limiting process observed in this study

Figure 10 portrays the temporal change in atmospheric CO_2 concentration from its initial value within the closed box in the flow-through type experiments for different combinations of andosol and Ca-rich silicate material. The initial CO_2 concentrations in the experiments conducted using andosol, without and with Portland cement, steel making slag, and coal fly ash were 460, 560, 460, and

500 ppm, respectively. In the experiment conducted using andosol alone, the decrease in the CO₂ concentration ceased within 60 min, resulting in a small reduction of 20 ppm. In contrast, in the experiment conducted using andosol with Ca-rich silicate material, the CO₂ concentration decreased continuously throughout the 600-min (10-h) experiment, achieving a larger reduction (>100 ppm). The change in the CO₂ concentration was highly nonlinear for all conditions; most changes occurred within the first 360 min (6 h), achieving stability with time. Additionally, the CO₂ concentration change reduction extent can be arranged in increasing order: cement, fly ash, and slag.

3.3 Behavior of atmospheric CO₂ removal process

Figure 11 portrays the changes in the TOC, IC, and Ca and Si concentrations in and pH of the effluents in the flow-through type experiments conducted in an unclosed box (as a function of total water addition). Notably, water was added at 10:00 and 16:00, with the time interval being 6 h at the maximum. This means fresh water was added after the point when atmospheric CO₂ removal by preexisting water almost ceased, based on the results of the previous section (Figure 11).

The pH values of the effluents obtained from the experiments conducted using andosol mixed with Portland cement, steelmaking slag, and coal fly ash were generally higher than those conducted using andosol alone (Figure 11A), wherein the pH tended to be larger (in the order of cement, slag, and fly ash), which was consistent with the results of the batch-type experiments (Runs 2–5). The IC in the experiment conducted using andosol alone portrayed a consistent trend, generally smaller than that observed in the experiments conducted using andosol and silicate materials (Figure 11B). In the experiments conducted using andosol and silicate materials, the IC first increased, until 300 ml of total water was added, followed by a decrease. Moreover, the order of magnitude of the IC was not constant throughout the experiment. There was no clear relationship between the changes in the pH and IC of the effluents. Nevertheless, the sum of the product of each IC value and the added water amount (0.1 L) differed (cement: ca. 8.6 mg, slag: ca. 8.0 mg, fly ash: ca. 6.9 mg). Therefore, the total CO₂ removal tended to be larger for a higher Ca content (or higher pH). The changes in TOC also had no clear relationship with the changes in pH (Figure 11C). In contrast, the Ca and Si concentrations showed a general decreasing trend, and were thus related to the pH; this reflected the consumption of Ca-rich materials, with increasing total water addition, due to dissolution.

It was not difficult to understand the reason for the overall changes in the pH and the Ca and Si concentrations of the effluents, all of which were caused primarily by the reaction between water and Ca-rich silicate materials distributed uniformly on the soil surface. In contrast, it was quite difficult to understand the reason for the overall changes in the IC and

TOC, which were primarily caused by the reactions between water and air and water and soil grains within pore spaces, despite the fact that the IC and TOC concentrations tended to be larger at higher pH, as demonstrated in the batch-type experiments (Figure 9). Empirically, the flow of water in the experiments conducted using slag and fly ash decreased with increasing water (that was added to promote dissolution), compared to that in the experiment conducted using cement, in which higher IC values were observed in the later stages of the experiment. This implies the importance of the spatially variable distribution of the gas phase and the corresponding distribution of the liquid phase, owing to the intermittently occurring air–water two-phase flows in soils.

4 Discussion

The batch experimental results in this study infer that the use of Ca-rich silicate byproducts facilitates the capture of atmospheric CO₂ in both the andosol and DG soil systems, due to the pH increase caused by silicates dissolution. However, in andosol, due to the high humic acid content in the pore water, the Ca²⁺ released from cement was immediately trapped through the cations exchange effect. The exchange of Ca²⁺ with H⁺ in humic acid contributes to the released of H⁺ into solution, restoring the pH of the solution to neutral and avoiding the precipitation of CaCO₃, as evidenced by TG measurement. The released of humic acid from andosol soil under alkaline condition, as confirmed by TOC and TG measurements, may also enhance the migration of Ca. Conversely, in DG soil with less humic acid, the Ca²⁺ released from cement reacted with dissolved CO₂ to generate carbonates.

In the flow-through type experiments, the trend of CO₂ concentration change shown in Figure 10 indicated that atmospheric CO₂ was removed by the dissolution in the soil pore water, with an elevated pH that resulted from the dissolution of Ca-rich silicate material. Based on the results of the batch-type experiments, a large pH increase occurred immediately after the initiation of the contact between water and the Ca-rich materials, and the continuous decrease in the CO₂ concentration demonstrated that the gas-phase diffusive transport of CO₂ (from the atmosphere into the air-filled pore spaces) in the soil samples was the rate-limiting process of atmospheric CO₂ removal. Additionally, the nonlinear changes in the CO₂ concentration for all conditions indicated that the diffusive transport of CO₂ occurred in an unsteady state.

This study also demonstrated that the absorption behavior of atmospheric CO₂ by soil pore water cannot be predicted based only on the average changes in the chemistry of the pore water (such as pH), while neglecting the spatially variable distribution of the gas phase and the corresponding distribution of the liquid phase, owing to the unsteady-state air–water two-phase flow. As shown in Section 3.2, the unsteady-state gas-phase diffusive transport of CO₂ from the atmosphere into the air-filled pore spaces in soils is a rate-limiting process of atmospheric CO₂ removal. To maximize CO₂ removal in

croplands *via* the enhanced weathering of Ca-rich industrial byproducts, it is necessary to better understand the gas-phase diffusive transport behavior of CO₂ from the atmosphere to the soil and through the soil; notably, this process is affected by the size and spatial distributions of gas-filled pore spaces in the soil, developed by unsteady-state air–water two-phase flow, due to intermittently occurring rainfall, all of which were not considered in the previous study (Beerling et al., 2020).

Furthermore, in the natural environment, the compositions of terrestrial rain could be complicated and vary significantly from place to place because the regional geology and human activities can greatly affect the types of particulates that get added to the atmosphere. The presence of sources of gaseous acids (SO₃, NO₂) and bases (NH₃) may contribute to Ca-rich silicate byproducts dissolution and affect atmospheric CO₂ dissolution, while the presence of metal ions may occupy the position in pore water of agriculture soil for Ca capture. Finally, before applying the system, the potential risks from the use of industrial byproducts, which may contain potentially toxic elements, to human and agriculture should be clarified. All the above factors may influence the experimental results and should be further investigated for practical application of the system.

5 Conclusion

In previous studies, enhanced weathering of industrial Ca-rich silicate byproducts in croplands has been suggested for large-scale profitable atmospheric CO₂ removal, through 1D vertical reactive transport model simulation (Beerling et al., 2020). However, considering the lack of realism of this model, in this study, we attempted to clarify the effectiveness and characteristics of such CO₂ removal systems and illuminate the dynamic influences of soils on fluid chemistry, such as kinetics of pH buffering and cation exchange, through batch-type and flow-through type laboratory experiments.

Experimental results suggest that agricultural soils, such as andosol are suitable for CO₂ removal as they provide moderately high pH and Ca concentrations in pore water, which can prevent intensive carbonate mineral precipitation. The IC concentration in the batch experiment conducted using andosol and cement was 3.1 times higher than that conducted using andosol alone. The flow-through experiments conducted in this study, using intermittent vertical water flow, indicated that greater atmospheric CO₂ removal (>100 ppm) may be expected for materials having higher Ca content. However, the magnitude of CO₂ removal and its time-dependent behavior are difficult to predict because they have no clear relation to the changes in the average pH value of soil pore water, probably due to the unexpectedly complex unsteady-state diffusive transport of CO₂ from the atmosphere-soil interface to deeper soils; notably, this is a rate-limiting process. To maximize atmospheric CO₂ removal in croplands *via* the enhanced weathering of industrial Ca-rich silicate byproducts, further studies are required to better understand the diffusive transport of CO₂ through gas-

filled pore spaces. Notably, the diffusive nature of the transport is created by the unsteady-state air–water two-phase flow resulting from intermittently occurring rainfall.

Data availability statement

The raw data supporting the conclusions of this article will be made available by the authors, without undue reservation.

Author contributions

KN and NW: conceptualization. RY and KN: data curation. RY and RS: formal analysis. KN, NW, and JW: funding acquisition. RY, KN, and NW: investigation. RY and KN: methodology. KN and NW: project administration. RY and KN: resources. RY and KN: software and writing-original draft. NW and JW: writing-reviewing and editing. All authors contributed to the article and approved the submitted version.

Funding

This study was partially supported by the Japan Society for the Promotion of Science (JSPS) through Grants-in-Aid for Scientific Research (B) (no. 22H02015), Challenging Research (Pioneering) (no. 21K18200), Early-Career Scientists (no. 21K14571), and Scientific Research (S) (no. 22H04932). This study was also supported by the Japan Science and Technology Agency (JST) and the Japan International Cooperation Agency (JICA) through JST/JICA Science and Technology Research Partnership for Sustainable Development (SATREPS) program (no. JPMJSA1703), by the Sumitomo Foundation through the Grant for Environmental Research Projects (no. 203137). The authors declare that this study received funding from Asahi Group Foundation, Ltd. through the Grant for Scientific Research Projects. This funder was not involved in the study design, collection, analysis, interpretation of data, the writing of this article, or the decision to submit it for publication.

Acknowledgments

We would like to thank Shinichi Yamasaki at the Graduate School of Environmental Studies, Tohoku University, for their assistance during the ICP-OES analyses.

Conflict of interest

The authors declare that the research was conducted in the absence of any commercial or financial relationships that could be construed as a potential conflict of interest.

Publisher's note

All claims expressed in this article are solely those of the authors and do not necessarily represent those of their affiliated

organizations, or those of the publisher, the editors and the reviewers. Any product that may be evaluated in this article, or claim that may be made by its manufacturer, is not guaranteed or endorsed by the publisher.

References

- Abdel-Gawwad, H. A., Metwally, A. K., and Tawfik, T. A. (2021). Role of barium carbonate and barium silicate nanoparticles in the performance of cement mortar. *J. Build. Eng.* 44, 102721. doi:10.1016/j.jobbe.2021.102721
- Bach, L. T., Gill, S. J., Rickaby, R. E. M., Gore, S., and Renforth, P. (2019). CO₂ removal with enhanced weathering and ocean alkalinity enhancement: Potential risks and co-benefits for marine pelagic ecosystems. *Front. Clim.* 1, 1–21. doi:10.3389/fclim.2019.00007
- Baqay, M. A., Li, J.-Y., Shi, R.-Y., Kamran, M. A., and Xu, R.-K. (2018). Higher cation exchange capacity determined lower critical soil pH and higher Al concentration for soybean. *Environ. Sci. Pollut. Res.* 25, 6980–6989. doi:10.1007/s11356-017-1014-y
- Beerling, D. J., Kantzas, E. P., Lomas, M. R., Wade, P., Eufrazio, R. M., Renforth, P., et al. (2020). Potential for large-scale CO₂ removal via enhanced rock weathering with croplands. *Nature* 583, 242–248. doi:10.1038/s41586-020-2448-9
- Beerling, D. J., Leake, J. R., Long, S. P., Scholes, J. D., Ton, J., Nelson, P. N., et al. (2018). Farming with crops and rocks to address global climate, food and soil security. *Nat. Plants* 4, 138–147. doi:10.1038/s41477-018-0108-y
- Dai, Y., Qiao, X., and Wang, X. (2018). Study on cation exchange capacity of agricultural soils. *IOP Conf. Ser. Mat. Sci. Eng.* 392, 042039. doi:10.1088/1757-899X/392/4/042039
- Das, S., Kim, G. W., Hwang, H. Y., Verma, P. P., and Kim, P. J. (2019). Cropping with slag to address soil, environment, and food security. *Front. Microbiol.* 10, 1320. doi:10.3389/fmicb.2019.01320
- Goll, D. S., Ciais, P., Amann, T., Buermann, W., Chang, J., Eker, S., et al. (2021). Potential CO₂ removal from enhanced weathering by ecosystem responses to powdered rock. *Nat. Geosci.* 14, 545–549. doi:10.1038/s41561-021-00798-x
- Green, J. K., Seneviratne, S. I., Berg, M., Findell, K. L., Hagemann, S., Lawrence, D. M., et al. (2019). Large influence of soil moisture on long-term terrestrial carbon uptake. *Nature* 565, 476–479. doi:10.1038/s41586-018-0848-x
- Hansen, J., Sato, M., Kharecha, P., von Schuckmann, K., Beerling, D. J., Cao, J., et al. (2017). Young people's burden: Requirement of negative CO₂ emissions. *Earth Syst. Dyn.* 8, 577–616. doi:10.5194/esd-8-577-2017
- Humphrey, V., Berg, A., Ciais, P., Gentile, P., Jung, M., Reichstein, M., et al. (2021). Soil moisture-atmosphere feedback dominates land carbon uptake variability. *Nature* 592, 65–69. doi:10.1038/s41586-021-03325-5
- Intergovernmental Panel on Climate Change (IPCC) (2018). *Global warming of 1.5 °C*. Geneva, Switzerland: World Meteorological Organization.
- Jorat, M. E., Goddard, M. A., Manning, P., Lau, H. K., Ngeow, S., Sochi, S. P., et al. (2020). Passive CO₂ removal in urban soils: Evidence from brownfield sites. *Sci. Total Environ.* 703, 135573. doi:10.1016/j.scitotenv.2019.135573
- Kantola, I. B., Masters, M. D., Beerling, D. J., Long, S. P., and DeLucia, E. H. (2017). Potential of global croplands and bioenergy crops for climate change mitigation through deployment for enhanced weathering. *Biol. Lett.* 13, 20160714. doi:10.1098/rsbl.2016.0714
- Kimura, T., and Koga, N. (2011). Monohydrocalcite in comparison with hydrated amorphous calcium carbonate: Precipitation condition and thermal behavior. *Cryst. Growth Des.* 11, 3877–3884. doi:10.1021/cg200412h
- Klemettinen, L., Avarmaa, K., Jokilaakso, A., and Taskinen, P. (2021). Iron activity measurements and spinel-slag equilibria in alumina-bearing iron silicate slags. *J. Alloys Compd.* 855, 157539. doi:10.1016/j.jallcom.2020.157539
- Lam, L., Wong, Y. L., and Poon, C. S. (2000). Degree of hydration and gel/space ratio of high-volume fly ash/cement systems. *Cem. Concr. Res.* 30, 747–756. doi:10.1016/S0008-8846(00)00213-1
- Madeira, M., Auxtero, E., and Sousa, E. (2003). Cation and anion exchange properties of Andisols from the Azores, Portugal, as determined by the compulsive exchange and the ammonium acetate methods. *Geoderma* 117 (3–4), 225–241. doi:10.1016/S0016-7061(03)00125-3
- Nelson, P. N., and Su, N. (2010). Soil pH buffering capacity: A descriptive function and its application to some acidic tropical soils. *Soil Res.* 48, 201–207. doi:10.1071/SR09150
- Rao, C., Guo, X., Li, M., Sun, X., Lian, X., Wang, H., et al. (2019). *In vitro* preparation and characterization of amorphous calcium carbonate nanoparticles for applications in curcumin delivery. *J. Mat. Sci.* 54, 11243–11253. doi:10.1007/s10853-019-03686-3
- Rockström, J., Gaffney, O., Rogelj, J., Meinshausen, M., Nakicenovic, N., and Schellnhuber, H. J. (2017). A roadmap for rapid decarbonization. *Science* 355, 1269–1271. doi:10.1126/science.aah3443
- Russell, A. E., Laird, D., and Mallarino, A. P. (2006). Nitrogen fertilization and cropping system impacts on soil quality in Midwestern mollisols. *Soil Sci. Soc. Am. J.* 70, 249–255. doi:10.2136/sssaj2005.0058
- Schmidt, M. P., Iltott, A. J., Phillips, B. L., and Reeder, R. J. (2014). Structural changes upon dehydration of amorphous calcium carbonate. *Cryst. Growth Des.* 25, 938–951. doi:10.1021/cg401073n
- Terrer, C., Phillips, R. P., Hungate, B. A., Rosende, J., Pett-Ridge, J., Craig, M. E., et al. (2021). A trade-off between plant and soil carbon storage under elevated CO₂. *Nature* 591, 599–603. doi:10.1038/s41586-021-03306-8
- Torrent, J., DelCampillo, M. C., and Barrón, V. (2015). Short communication: Predicting cation exchange capacity from hygroscopic moisture in agricultural soils of Western Europe. *Span. J. Agric. Res.* 13 (4), e11SC01. doi:10.5424/sjar/2015134-8212
- Wang, J., Watanabe, N., Inomoto, K., Kamitakahara, M., Nakamura, K., Komai, T., et al. (2022). Sustainable process for enhanced CO₂ mineralization of calcium silicates using a recycling agent under alkaline conditions. *J. Environ. Chem. Eng.* 10, 107055. doi:10.1016/j.jece.2021.107055
- Wuenschel, R., Unterfrauner, H., Peticzka, R., and Zehetner, F. (2015). A comparison of 14 soil phosphorus extraction methods applied to 50 agricultural soils from Central Europe. *Plant Soil Environ.* 61, 86–96. doi:10.17221/932/2014-PSE
- Zeng, S., Liu, Z., and Groves, C. (2022). Large-scale CO₂ removal by enhanced carbonate weathering from changes in land-use practices. *Earth. Sci. Rev.* 225, 103915. doi:10.1016/j.earscirev.2021.103915
- Zhang, G., Kang, J., Wang, T., and Zhu, C. (2018a). Review and outlook for agronomical research in agriculture and climate mitigation. *Soil Res.* 56, 113–122. doi:10.1071/SR17157
- Zhang, J., Zhou, X., Dong, C., Sun, Y., and Yu, J. (2018b). Investigation of amorphous calcium carbonate's formation under high concentration of magnesium: The prenucleation cluster pathway. *J. Cryst. Growth* 494, 8–16. doi:10.1016/j.jcrysgro.2018.05.001